Available online at www.sciencedirect.com
SCIENCE DIRECT
Catalysis Today 102–103 (2005) 133–141
CATALYSIS TODAY
www.elsevier.com/locate/cattod

Microwave plasma assisted preparation of Pd-nanoparticles with controlled dispersion on woven activated carbon fibres

Pavel Korovchenko, Albert Renken, Lioubov Kiwi-Minsker *

Ecole Polytechnique Fédéral de Lausanne, LGRS-EPFL, CH-1015 Lausanne, Switzerland

Available online 31 March 2005

Abstract

The low-pressure cold microwave (MW) plasma is shown as an efficient method to increase acidity of the ACF within less than 1 min treatment without affecting the fibre morphology and strength. The ion-exchange capacity was 1.6 times higher compared to the non-treated ACF sample. Selective removal of the carboxylic groups from the ACF surface by the air–MW-plasma allows to keep the phenolic groups intact. Palladium was deposited on ACF from $[Pd(NH_3)_4]Cl_2$ solution via ion-exchange with the protons of the phenolic surface groups. Surface phenolic groups were able to chemically anchor Pd in cationic form, leading after reduction in H_2 to small Pd° nanoparticles (<3 nm). The Pd dispersion was measured by CO pulse adsorption and confirmed by the TEM analysis. Heating of the Pd/ACF catalysts in H_2 at 573–773 K is necessary to reduce Pd(II) to Pd°. This reduction can be also achieved by the H_2–MW-plasma treatment in less than 1 min with the corresponding saving of energy.

Keywords: Activated carbon fibres; Pd nano-particles; Cold micro-wave plasma; Surface functional groups; TPD analysis

1. Introduction

Activated carbon fibres (ACF) in the form of woven fabrics recently have been shown as suitable catalytic supports for noble metals [1–5]. These materials have high specific surface area up to 3000 m^2/g and allow high loading of metal nano-particles ensuring an increased specific activity. To achieve high metal dispersion, the carbon fabric requires a pre-treatment to increase the concentration of the surface functional groups. These pre-treatments like gas-phase oxidation by CO_2 or O_2, steaming or wet chemical oxidation by H_2O_2, HNO_3, $KMnO_4$, NaOCl and $(NH_4)_2S_2O_8$ have been carried out with different carbons leading to the formation of oxygen containing groups like carboxyl, carbonyl, phenol, quinone and lactones on the carbon surface [6–10]. In a previous publication [11] it was shown that phenolic groups were responsible for the high dispersion of noble metals (Pd, Pt or Au) on ACF deposited by cationic ion-exchange from aqueous solutions of the metal ammonia complexes. Carboxylic surface groups on ACF fabrics were observed to lead to the formation of relatively big (>10 nm) metal particles, while surface phenolic groups were able to chemically anchor gold ions that after reduction in H_2 lead to small Au° nanoparticles (<5 nm) on ACF. The surface groups can be controlled via selective decomposition by heating in an inert atmosphere [11–14]. However, the traditional pre-treatments are time and energy consuming and often damage the surface of carbon materials. This is especially important in the case of the ACF due to the specific morphology of carbon fibres, which should be preserved.

During the last 10 years low temperature plasma techniques have been applied for the surface modification of carbons. Microwave (MW) plasma is used at temperatures as low as room temperature. This allows treating carbon surfaces to meet specific requirements without affecting the fibre textural characteristics and strength.

Thus, Boudou et al. [15] confirmed by SEM and STM analysis that the pitch-based carbon fibres treated in low pressure (1.0 mbar) oxygen MW plasma during 1–5 min keep their structure and diameter. At the same time, the carbon surface is cleaned from contaminations and the specific surface area (SSA) is increased due to improved roughness.

* Corresponding author. Tel.: +41 21 693 31 82.
E-mail address: lioubov.kiwi-minsker@epfl.ch (L. Kiwi-Minsker).

0920-5861/$ – see front matter © 2005 Elsevier B.V. All rights reserved.
doi:10.1016/j.cattod.2005.02.019

The type of gas used for MW-plasma treatment is known to affect the surface modification. For example, oxygen or air plasma leads to the oxidation of carbon surface [15–27]. Nitrogen and ammonia plasmas introduce C/N functionality on carbon surface [26–28]. Argon plasma activates the carbon surface due to etching and "cleaning" processes [29–31]. Hydrogen plasma has been used for the cleaning of carbons to improve the SSA [28]. Moreover, it is possible to obtain different surface effects by varying the plasma parameters (power, treatment time, and gas pressure) without changing the gas. For example, oxygen or air MW-plasma creates on the carbon surface oxygen containing groups under low power treatment within short time [15,26,27], but cleans the surface with the partial elimination of the oxygen functionality under high power MW radiation during long exposures [15,22].

Cold MW plasma has been rarely applied for the preparation of catalytically active particles of noble metals on various carriers. The only reports found concern the formation of Pt and Au nanoparticles in zeolites [32–34].

In this study, cold MW-plasma under oxygen, air or hydrogen at low pressure was applied for the surface modification of ACF woven fabrics. The selective regulation of the surface functionality to control the dispersion of Pd nano-particles deposited via ion-exchange/adsorption from different Pd-containing precursors was the aim of this work. It is well known that the catalyst post-treatment is necessary for metal complex decomposition and metal particles activation. The high temperature reduction by hydrogen is used for this purpose leading to the metal sintering with a decrease in the observed catalytic activity. The high reductive capacity of cold plasma under H_2 has been reported [32,33,35]. The catalyst post-treatment by oxygen cold plasma is also known for the precursor complex destruction [34,36]. In this work, the O_2 and H_2 MW-plasma catalyst post-treatment is further investigated in detail. We present hereby the first evidence on the MW-plasma assisted preparation of structured Pd/ACF catalysts where the combination of the support pre-treatment with the catalyst post-treatment by cold MW-plasma is used for the controlling of Pd dispersion.

2. Experimental

2.1. Materials

The ACF of polyacrylonitrile (PAN) in the form of plain woven fabrics (AW1101, KoTHmex, Taiwan Carbon Technology Co.) were used as supports. The fabrics are woven from the long threads of ca. 0.5 mm in diameter consisting of a bundle of elementary filaments of 3–5 μm in diameter. The elemental composition of the ACF was >99.9% of carbon as measured by atomic absorption spectroscopy (AAS). The tetra-ammine-palladium(II) chloride monohydrate $[Pd(NH_4)_3]Cl_2{\cdot}H_2O$ "p.a." was used as received (Aldrich Chem. Co., Reactolab S.A., Switzerland). The palladium(II) chloride anhydrous ($PdCl_2$) and the sodium chloride (NaCl) were "p.a." from Fluka (Buchs, Switzerland). The Na_2PdCl_4 was prepared by mixing equivalent amounts of $PdCl_2$ and NaCl in aqueous solution. All gases in this study were >99.9998% (CarbaGas, Switzerland).

2.2. Modification of the ACF support

2.2.1. The ACF treatment by MW-plasma

The ACF treatment by MW-plasma was performed with the MW-plasma apparatus of Vacotec Swiss Co. and used at 2.45 GHz. The power was varied from 100 to 600 W, the reaction times were changed from 10 to 180 s, the gas flow was between 20 and 100 ml/min, and the gas pressure varied from 0.02 to 2 mbar. Before the sample treatments the plasma MW-chamber was evacuated for 2 h up to 0.001 mbar. The MW-plasma in oxygen (O_2–MW-plasma) and MW-plasma in air (air–MW-plasma) were used to oxidize the ACF surface. The MW-plasma in hydrogen (H_2–MW-plasma) was applied to replace the traditional high temperature reduction of Pd-ions by H_2.

The ACF without any treatment is denoted as $ACF_{original}$. Two ACF samples treated in a traditional way were used for the comparison of the textural and surface chemical properties with the plasma-treated ACF. One sample, ACF_{HNO_3}, was boiled in aqueous HNO_3 (15 vol.%) for 1 h, rinsed with distilled water until neutral pH, air–dried for 3 h at room temperature and finally for 15 h at 393 K. The sample $ACF_{He,1273}$ was obtained by heating the $ACF_{original}$ in He (1273 K, 100 ml/min, 1 h).

2.3. Preparation of Pd/ACF catalysts

Pd deposition was performed via ion-exchange/adsorption from two different precursors. The ACF fabrics (∼1.6 g) were immersed in stirred $[Pd(NH_4)_3]Cl_2$ or Na_2PdCl_4 aqueous solutions for 5 h. The pH of the solution was kept neutral without any alkali addition. The Pd concentrations were varied from 1 to 5 wt.%. After Pd-ions deposition, the fabrics were rinsed with distilled water, air-dried for 3 h at room temperature and finally for 15 h at 393 K.

2.3.1. Pd/ACF catalysts activation

Pd/ACF catalysts activation was carried out by MW-plasma post-treatment in oxygen or hydrogen in order to eliminate ammonium or chlorine-ions present in Pd complex. The MW-plasma treatment was used as described in Section 2.2. In order to prevent the Pd particles sintering, the MW-plasma oxidative post-treatment was performed in four consecutive cycles for 15 s spaced 5 min apart.

2.4. Catalysts characterization

2.4.1. The specific surface areas

The SSA were measured using N_2 adsorption–desorption at 77 K by a Sorptomatic 1990 instrument (Carlo Erba). The

samples were heated in vacuum at 523 K for 2 h before the measurements. The SSA of the samples was calculated employing the BET method. The Dollimore/Heal method was applied for pore volume and pore-size calculation. The pore size distribution was in the range between 1 and 9 nm suggesting a micro- and meso-porosity for the examined materials.

2.4.2. The temperature programmed decomposition (TPD) in He

The TPD in He was carried out to identify the surface functional groups and for characterization of surface acidity using a Micromeritics AutoChem 2910 analyzer. For the TPD measurements 0.05 g of ACF sample was placed in a quartz plug-flow reactor and purged in He flow (20 ml/min) for 30 min at room temperature. Then, the temperature was increased up to 1273 K with a ramp of 10 K/min. The control of a reaction temperature was performed by a thermocouple placed in the catalytic bed. The TPD products were analyzed by ThermoStar-200 quadrupole ''on-line'' mass-spectrometer (Pfeiffer Vacuum) calibrated with gas mixtures of known compositions. The intensity of the following peaks was measured simultaneously: 2, 4, 15, 18, 28, 30, 32 and 44 m/e.

2.4.3. XPS analysis

XPS analysis by Axic Ultra ASCA system (Kratos, Manchester) with monochronated Al Kα radiation (1486.6 eV) and an X-ray power of 150 W was used to determin the surface chemical composition.

2.4.4. The atomic absorption spectroscopy

The atomic absorption spectroscopy was carried out via Shimadzu AA-6650 with air–acetylene flame. The amount of deposited Pd was controlled by the analysis of the residual solution of Pd precursor and by chemical analysis of the Pd/ACF samples. For the chemical analysis the Pd/ACF samples were heated in air at 973 K for 2 h in order to burn out the carbon and the obtained ashes (<0.1 wt.%) were dissolved in hot aqua regia containing HF.

2.4.5. The SSA of Pd and its dispersion

The SSA of Pd and its dispersion were measured by CO pulse adsorption (3 vol.% CO in He) at 323 K using a Micromeritics AutoChem 2910 analyzer. The samples (0.05 g) were pre-treated in a flow of He (100 ml/min) at 423 K during 1 h and subsequently in H_2 (100 ml/min) flow at 423 K during 1 h. A Pd density of 12.02 g/cm^3 and a stoichiometry factor SF_{Pd} = CO/Pd of 1.667 were taken for the SSA_{Pd} calculation.

2.4.6. The high resolution transmission electron microscopy (HRTEM)

The high resolution transmission electron microscopy was used for the investigation of surface morphology via Philips CM300UT FEG with 300 kV field emission gun, 0.65 mm spherical aberration and 0.17 mm resolution at Scherzer defocus. The images were recoded on a Gatan 797 slow-scan CCD camera (1024 × 1024 pixels) and processed with theGatan Digital Micrograph 3.4.4 software to measure the distances and the angles between the atomic planes.

3. Results and discussion

3.1. Effect of MW-plasma treatment on ACF texture

One of the objectives of the present study is to modify by cold MW-plasma the textural characteristics of ACF fabrics and their surface functionality. The effect of different pre-treatments on the SSA of ACF supports is presented in Table 1. The SSA is seen to depend strongly on the treatment varying from 600 to 1050 m^2/g. The liquid phase oxidation by boiling HNO_3 decreases the SSA of the $ACF_{original}$ sample from 925 to 613 m^2/g. This indicates that the ACF surface oxidation leads to the decrease in micropores when introducing oxygen functionality. These observations agree with the reported results [37,38]. ACF treatment in He at 973 K and at 1273 K during 1 h slightly decreases the SSA from 925 to ∼820 m^2/g. This suggests partial surface destruction due to higher temperatures. In contrast, the MW-plasma treatments slightly increase the SSA if compared to the $ACF_{original}$ independently of the nature of the gas used. This may be explained by the surface cleaning with simultaneous opening of micro-pores at the external surface of the sample [15]. At the same time it is important to note that the internal structure of the sample meso- and micro-porosity is not modified by the plasma treatment, even under the conditions used for the high degree of the ACF burn-off [18].

The adsorption capacities for $[Pd(NH_3)_4]Cl_2$ complex on the ACF supports show in Table 1 that the surface functionality is strongly affected. Thus, in spite of the decreased porosity of the ACF_{HNO_3} sample as compared to the $ACF_{original}$, the amount of the Pd adsorbed is two-fold higher. The chemical properties of activated carbons are

Table 1
Specific surface area and adsorption capacity of the ACF supports after different pre-treatments

ACF supports	ACF treatment	Surface area B.E.T. (m^2/g)	Adsorption of Pd[a] (mmol/g)
$ACF_{original}$	No	925	0.13
ACF_{HNO_3}	Boiling in HNO_3	613	0.24
$ACF_{He,973}$	Heating in He at 973 K, 1 h	822	–
$ACF_{He,1273}$	Heating in He at 1273 K, 1 h		0.05
$ACF_{air–MW\text{-}plasma}$	Air–MW-plasma	1018	0.21
$ACF_{O_2–MW\text{-}plasma}$	O_2–MW-plasma	959	–
$ACF_{H_2–MW\text{-}plasma}$	H_2–MW-plasma	1049	–

[a] In the form of $[Pd(NH_3)_4]Cl_2$ complex.

known to be very important for the metal deposition because the adsorption capacity is determined by (a) porous structure and (b) by the chemical nature of the surface, in particular by the surface oxygen groups. Therefore, this question warrens a detail study.

3.2. Effect of MW-plasma treatment on ACF surface functional groups

It is well known that each type of surface oxygen group decomposes to the well defined products, e.g., that CO_2 derives from carboxyl, lactone/lactol and carboxyl anhydride groups, and CO is formed by decomposition of carboxyl anhydride, carbonyl/quinone, phenolic and ether-type oxygen groups [6,12]. Total amounts of CO and CO_2 produced during TPD analysis can be used for the quantitative and qualitative characterization of the carbon surface functional groups [6,7].

3.2.1. The influence of the gas nature applied during MW-plasma treatment

The influence of the gas nature applied during MW-plasma treatment on the ACF surface functionality was studied by TPD analysis. The ACF samples pre-treated by MW-plasma in air, O_2 and H_2 were compared with the ACF samples modified by HNO_3 and by He at high temperature. Fig. 1 presents the comparative bar diagram of total amounts of CO and CO_2 obtained during TPD. The HNO_3 wet oxidation produces ACF surfaces with a high total acidity. Thus, the total amount of CO_2 increases about 10 times and the total amount of CO is about 2.5-fold higher if compared with the $ACF_{original}$. The thermal treatment in inert atmosphere (He) completely eliminates the precursor groups leading to CO_2 evolution during TPD and drastically decreases the oxygen species able to produce CO. The same tendency is observed also for the sample of ACF treated by O_2–MW-plasma (600 W, 0.2 mbar, 30 s). In contrast to this, the H_2–MW-plasma treatment (600 W, 0.5 mbar, 30 s) gives the biggest SSA and does not change the surface functionality. The results obtained for air–MW-plasma treatment are the most interesting. In this case, the total amount of CO_2 increases two times as compared to $ACF_{original}$ sample, but the amount of CO evolved is about four times higher than that of the original sample. This indicates the selective destruction/creation of surface oxygen groups by air–MW-plasma treatment, allowing the control of ACF surface functionality. Therefore, the air–MW-plasma treatment was optimized as seen below.

Table 2
Parameters of the air–MW-plasma treatment of the ACF-support and the amounts of CO and CO_2 evolved during TPD in He

	CO (mmol/g)	CO_2 (mmol/g)
Treatment time (s)		
15	3.16	0.52
30	3.26	0.55
60	3.20	0.54
Plasma power: 300 W, gas pressure: 0.2 mbar		
Gas pressure (mbar)		
0.01	3.20	0.48
0.2	3.26	0.55
Plasma power: 300 W, treatment time: 30 s		
Plasma power (W)		
150	2.31	0.45
300	3.26	0.55
600	3.94	0.57
Treatment time: 30 s, gas pressure: 0.2 mbar		

3.2.2. Optimisation of the air–MW-plasma parameters

Optimisation of the air–MW-plasma parameters was aimed on the regulation of the total amount of surface oxygen groups and the achieving chemical uniformity of the surface groups. The results are summarised in Table 2. The optimisation was carried out by varying the treatment time, the air pressure and the plasma power. The treatment time was limited by 1 min to avoid the ACF samples burn-of. The ACF sample oxidation by air–MW-plasma (300 W) was performed in air at 0.2 mbar varying the treatment times. By TPD analysis it was observed that the highest amount of CO producing groups corresponds to 30 s. The total amount of CO_2 was not changed with treatment time.

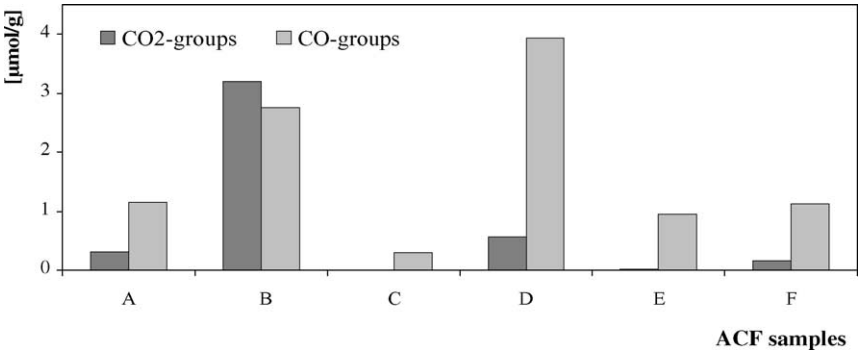

Fig. 1. Bar diagram of total amounts of CO_2 and CO obtained by TPD for different pre-treated ACF samples. (A) ACF original, (B) ACF treated in HNO_3, (C) ACF treated in He at 1273 K, (D) ACF treated in air–MW-plasma, (E) ACF treated in O_2–MW-plasma, and (F) ACF treated in H_2–MW-plasma.

This can be explained by the low stability of carboxylic groups which were probably destroyed within the first seconds of the treatment. The best result on variation of air pressure was obtained for the pressure of 0.2 mbar. At lower pressure of 0.01 mbar, the number of ionized reactive species was probably too low for the oxidation of ACF in 30 s [22]. On the other hand, our attempts to increase the air pressure up to 2 mbar failed due to the problems with plasma initiation and its stability. To optimise the plasma power, ACF samples were treated during 30 s under the air pressure of 0.2 mbar at 150, 300 and 600 W. The biggest amounts of CO and CO_2 producing groups correspond to the plasma power of 600 W, since an increased number and energy of ionised reactive species leads to a higher ACF surface oxidation.

3.2.3. The TPD profiles

The TPD profiles of non-treated and treated ACF samples were examined to understand the nature of surface oxygen groups contributing to the CO and CO_2 evolved during TPD runs. The results are presented in Fig. 2. The TPD profiles show that the groups producing CO_2 are less stable then the

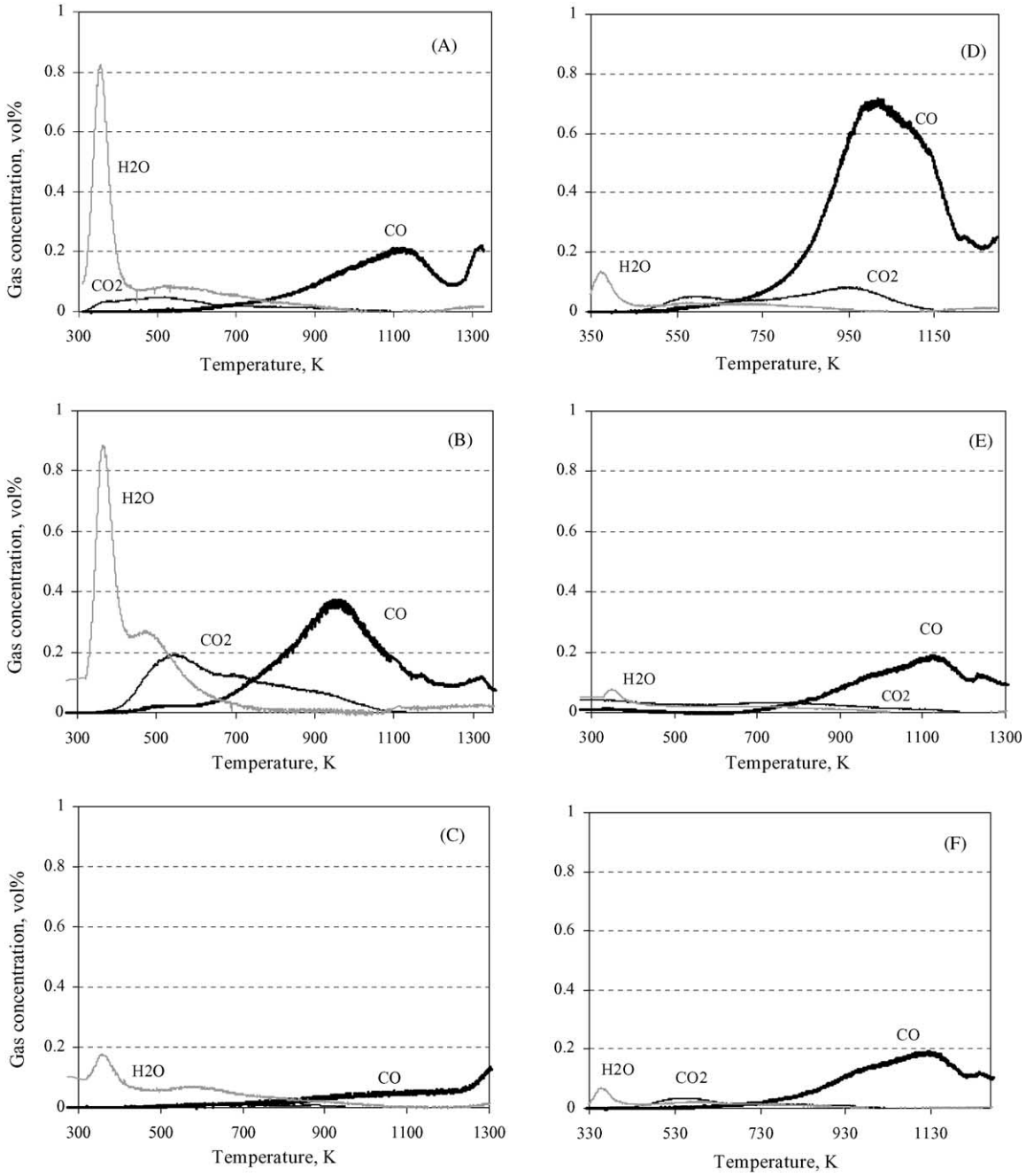

Fig. 2. TPD profiles of ACF samples (0.05 g, He: 20 ml/min, 10 K/min) after different pre-treatments. (A) ACF original, (B) ACF treated in HNO_3, (C) ACF treated in He at 1273 K, (D) ACF treated in air–MW-plasma, (E) ACF treated in O_2–MW-plasma, and (F) ACF treated in H_2–MW-plasma.

groups producing CO since they start to decompose at about 400 K. The profile of the non-treated $ACF_{original}$ sample (Fig. 2A) consists of CO_2 overlapping peaks with maxima at 350 and 540 K and of broad CO peak centered at about 1100 K. The first CO_2 peak accompanied by the high H_2O peak can be assigned to elimination of adsorbed CO_2 [12,15,16]. The CO_2 peak at 540 K, which is also accompanied by H_2O peak with maximum at 500 K, can be attributed to the carboxylic group's decomposition [6,11,39]. The left broad shoulder of the CO peak may correspond to the decomposition of phenolic groups, which is known to take place around 873–973 K. The maximum at 1100 K of the CO peak is assigned to the carbonyl and quinone groups' destruction [6,40].

The TPD profile of the ACF after HNO_3 wet oxidation is presented in Fig. 2B. It follows that the HNO_3 treatment increases the acidity of ACF surface. This is reflected in the increased amount of CO_x evolved besides the appearance of some new peaks. Thus, the presence in the CO_2 spectra of intensive peak at 540 K accompanied by H_2O peak as well as

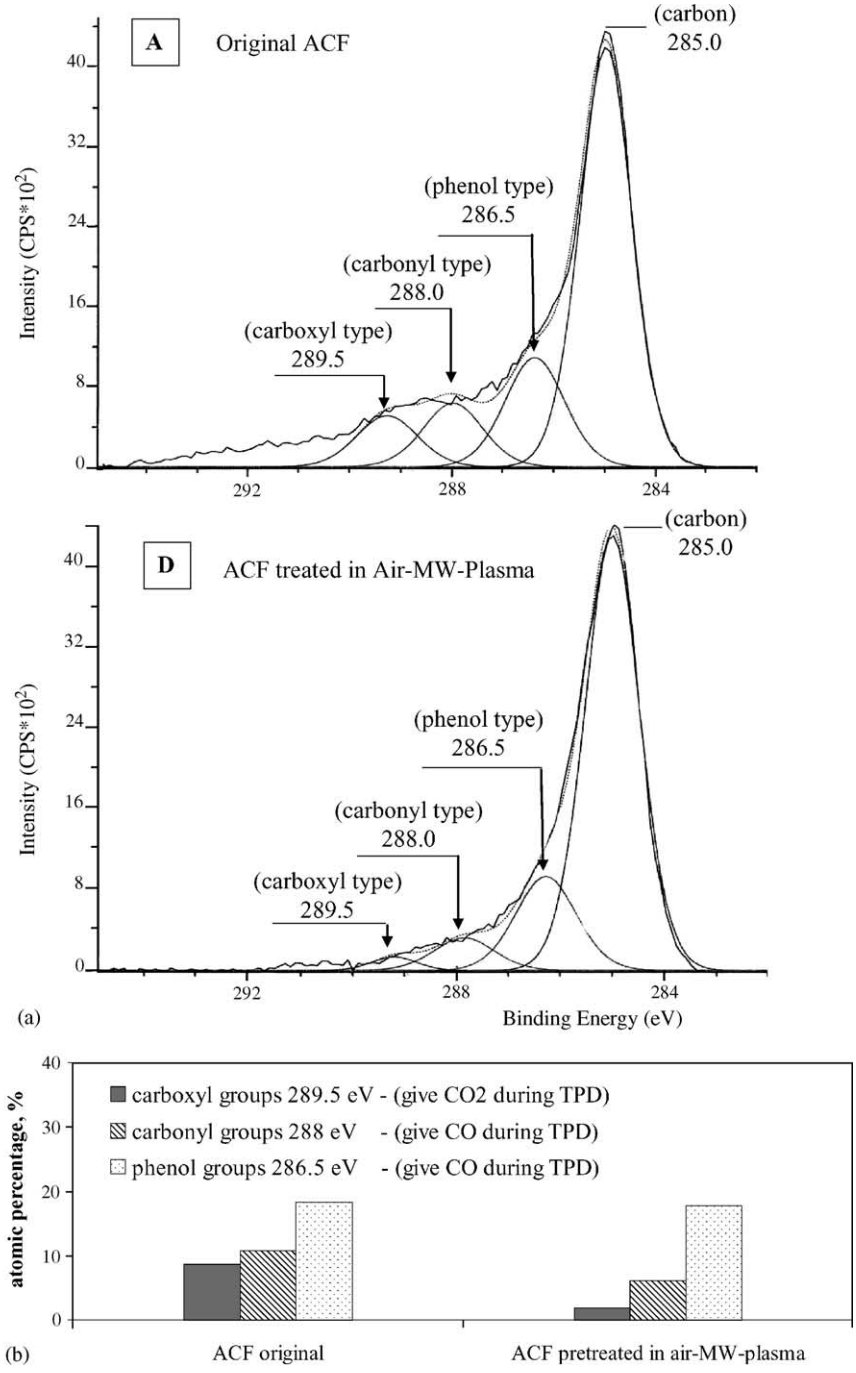

Fig. 3. (a) C1s XPS spectrums of original (A) and air–MW-plasma treated (D) ACF samples. (b) Bar diagram of the surface concentration of functional groups determined by XPS for non-treated and air–MW-plasma treated ACF samples.

the appearance of CO_2 peak at 900 K, can be caused by carboxylic group's decomposition at about 500 K with the formation of more stable carboxylic anhydride groups. The latter groups are known to decompose at about 700–870 K with simultaneous formation of CO and CO_2 [6,11,39]. The CO_2 peak observed at about 700 K indicates the presence of surface lactone oxygen groups [6,11,40,41]. At the same time the large symmetric CO peak centred at 950 K can be attributed to decomposition of carboxyl anhydride groups (700–870 K), phenolic (900 K) and carbonyl/quinone groups (1100 K) [6,11,40]. The TPD profile of the ACF sample treated in He at high temperature (Fig. 2C) confirms the almost complete elimination of oxygen containing functional groups during this treatment.

The TPD profile of air–MW-plasma treated ACF sample (Fig. 2D) is presented by the small CO_2 peak at 540 K (carboxylic groups) and 950 K (carboxyl anhydride groups) and by a broad intensive peak of CO with a maximum at ~950 K. This maximum is composed by CO derived from the decomposition of phenolic and carboxyl anhydride groups. At the same time the contribution of carboxyl anhydride groups in this CO peak cannot be significant considering the stoichiometry of CO and CO_2 produced from carboxylic anhydride groups. The high shoulder of CO at about 1130 K was attributed to the relatively thermostable carbonyl and quinone groups [6,11,39–41].

The TPD profiles of O_2–MW-plasma (Fig. 2E) and of H_2–MW-plasma (Fig. 2F) show CO peaks at 950 K (phenolic groups) and at 1130 K (carbonyl and quinone groups). The general trend of the CO TPD profiles obtained for O_2– and H_2–MW-plasma treated samples was similar to the profile of the non-treated $ACF_{original}$ sample. This contrasts the CO TPD profiles of the ACF treated in air–MW-plasma and of the ACF_{HNO_3} sample, which are different to the $ACF_{original}$. This fact suggests the different nature of surface oxygen groups.

3.2.4. XPS analysis

XPS analysis was used for the analyses of the ACF functionality [15,42,43] after different treatments. XPS spectra obtained for original and air–MW-plasma treated ACF samples (Fig. 3a(A and D)) reveal the carbon of graphitic type (285 eV), phenolic (286.5 eV), carbonyl (288 eV) and carboxylic (289.5 eV) groups. Moreover, the tendency of predominant phenolic groups on the ACF treated by MW-plasma, as seen by TPD, is further confirmed. At the same time, the relative amounts of different oxygen groups observed by XPS do not correspond to those found by TPD (see Fig. 3b). This discrepancy in the quantities of the surface functional groups obtained by XPS and TPD is due to the different thickness of the surface layer analyzed. XPS can penetrate up to a few nanometres, giving information involving the over layer (external surface) of the sample. The TPD reaches the whole sample volume [44]. Therefore, the comparison of XPS with the TPD results indicates the difference between the over layer in relation to the bulk of the material.

Table 3
Characteristics of the Pd/ACF catalysts prepared from Na_2PdCl_4 precursor

Catalyst	Palladium		Treatment	
	Dispersion (%)	*d* (nm)	Of the support	Of the catalyst[a]
5% Pd/ACF	63.0	1.8	Original	–
5% Pd/ACF	54.0	2.1	HNO_3	–
4% Pd/ACF	51.0	2.2	Air–MW-plasma	–
4%Pd/ACF	29.0	3.8	Air–MW-plasma	H_2–MW-plasma
4%Pd/ACF	27.0	4.0	Air–MW-plasma	O_2–MW-plasma

[a] Before reduction in H_2.

3.3. Deposition of Pd via ion-exchange

Two different Pd precursors were examined for the deposition. The Na_2PdCl_4 was used to anchor the Pd as anion. The $[Pd(NH_3)_4]Cl_2$ complex was used to deposit Pd in cationic form. The results obtained for the anionic complex of Pd are presented in Table 3. The air–MW-plasma causes the particles sintering decreasing the metal dispersion from 63%, in the case of non-treated sample, to 51% for air–MW-plasma treated ACF sample. The same trend was observed for the HNO_3 pre-treated ACF support (ACF_{HNO_3}). The attempt to apply the catalyst post-treatment in H_2– or O_2–MW-plasma to eliminate the traces of chloride ions results in the twofold increase of the diameters of Pd particles and in a concomitant 50% reduction in the Pd dispersion. This result indicates that MW-plasma under mild conditions is able to induce metal sintering.

The data obtained for the Pd deposition from the $[Pd(NH_3)_4]Cl_2$ complex are summarised in Table 4. The air–MW-plasma pre-treatment of ACF support doesn't influence the diameter and dispersion of the anchored Pd particles in comparison with Pd deposited on the ACF_{HNO_3} support. To form catalytically active dispersed metal, it is usually necessary to reduce the catalyst before reaction. In our case to decompose the anchored Pd cationic complex and to eliminate the ammonium traces, the catalyst post-treatment by O_2–MW-plasma was applied. In Table 4 it is shown that the diameter of Pd particles deposited on $ACF_{original}$ is strongly increased during the plasma treatment (the metal dispersion was reduced more than three times). This was not the case for the Pd/ACF catalyst prepared from the air–MW-plasma pre-treated support, since the change of the diameter

Table 4
Characteristics of the Pd/ACF catalysts prepared from $[Pd(NH_3)_4]Cl_2$ precursor

Catalyst	Palladium		Treatment	
	Dispersion (%)	*d* (nm)	Of the support	Of the catalyst[a]
2.5% Pd/ACF	41.0	2.7	Original	–
2.5% Pd/ACF	47.0	2.4	HNO_3	–
2.0% Pd/ACF	45.0	2.5	Air–MW-plasma	–
2.5% Pd/ACF	12.0	9.1	Original	O_2–MW-plasma
2.0% Pd/ACF	31.0	3.2	Air–MW-plasma	O_2–MW-plasma

[a] Before reduction in H_2.

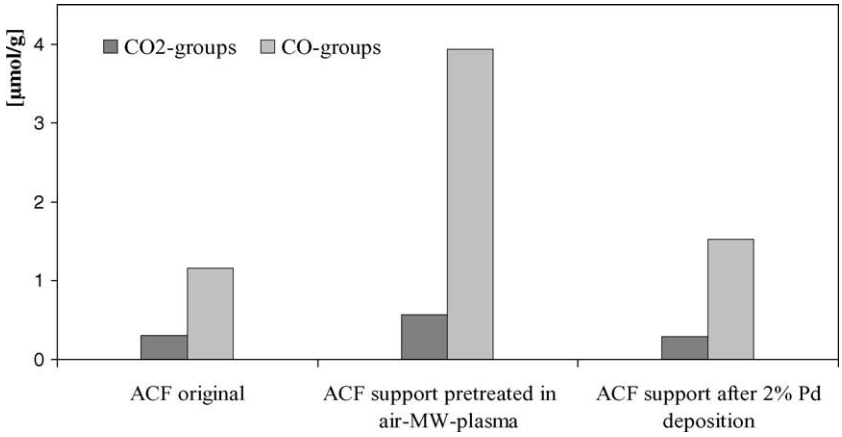

Fig. 4. Bar diagram of CO_2 and CO evolved during the TPD for the non-treated ACF, the air–MW-plasma pre-treated ACF and after Pd deposition on it from $Pt(NH_3)_4Cl_2$ complex.

of Pd particles was negligible and the high metal dispersion was retained. This result indicates a feasibility of air–MW-plasma pre-treatment for a high Pd dispersion on ACF.

Fig. 4 presents total amounts of CO and CO_2 formed during the TPD of non-treated $ACF_{original}$ support in comparison with the ACF pre-treated by air–MW-plasma before and after Pd deposition. As compared to the original ACF support, the surface acidity is strongly increased by the air–MW-plasma treatment and is presented by CO and CO_2 producing surface groups with the ratio of 6:1. The significant decrease of the surface acidity with a majority in CO producing groups is observed after Pd deposition. This indicates that Pd is anchored by ion-exchange with surface phenolic groups. It was shown [11] that phenolic groups contrary to carboxylic surface groups are responsible for the strong cation's anchoring to the carbon surface. The phenolic groups interact with the $[Pd(NH_3)_4]Cl_2$ precursor remaining their cationic form:

$$\copyright - OH + Pd^{2+} \rightarrow \copyright - O^{-}Pd^{2+} + H^{+}$$

At contrast, the interaction of $[Pd(NH_3)_4]Cl_2$ solution with the less stable carboxylic groups, leads to surface decarboxylation and reduction of Pd(II) to Pd(0):

$$\copyright - COOH + Pd^{2+} \rightarrow \copyright + Pd^{0} + H^{+} + CO_2\uparrow$$

During the reductive activation of the catalyst in H_2 at 573 K, the former particles serve as nucleation centers for the formation of bigger agglomerates upon surface migration, resulting in coalescence. Formation of big Pd agglomerates leads to a decline in metal dispersion and could be avoided applying cold MW-plasma. At low temperatures the sintering is less pronounced and high Pd dispersion is achieved. For 2%Pd/ACF catalyst a Pd dispersion of ~45% was obtained.

The TEM analysis confirms the Pd dispersion and shows the Pd clusters with a mean diameter of ~2.5 nm on the ACF supports (see Fig. 5).

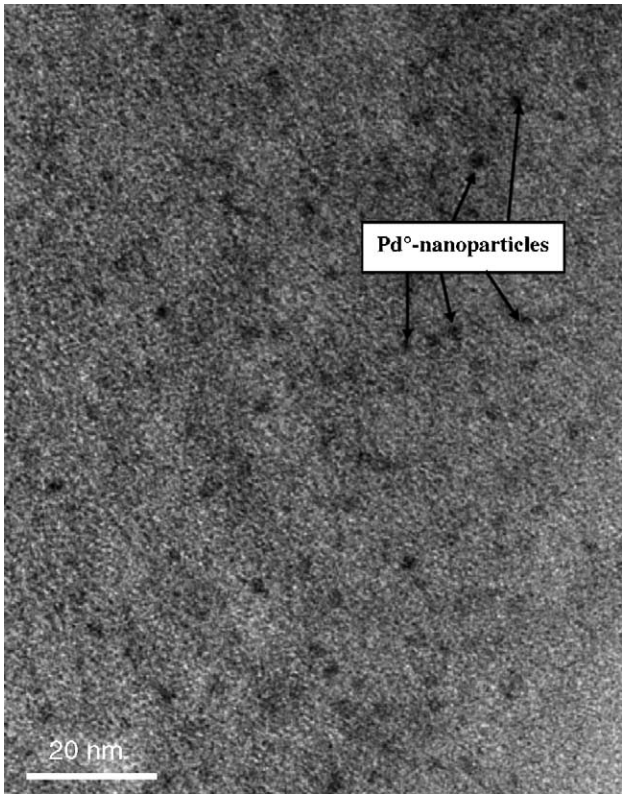

Fig. 5. HRTEM image of 2%Pd/ACF catalyst: the ACF support pre-treated in air–MW-plasma $[Pd(NH_3)_4]^{2+}$ complex decomposed in O_2–MW-plasma, the catalyst reduced in H_2 (100 ml/min, 373 K, 30 min).

4. Conclusions

1. The low-pressure air–MW-plasma is an efficient method of surface modification of the ACF increasing the surface acidity within less than 1 min treatment without affecting the fibre morphology and strength.
2. Selective removal of the carboxylic groups from the ACF surface by the air–MW-plasma allows keeping the

phenolic groups intact on the ACF surface ensuring Pd metal particles deposition with a high dispersion.

3. Palladium was deposited on ACF from $[Pd(NH_3)_4]Cl_2$ solution via ion-exchange with the protons of phenolic surface groups. Surface phenolic groups were able to chemically anchor Pd in cationic form, leading after reduction in H_2 to small Pd° nanoparticles (<3 nm).
4. Heating of the Pd/ACF catalysts in H_2 at 573–773 K is necessary to reduce Pd(II) to Pd°. This reduction can be also achieved by the H_2–MW-plasma treatment within 1 min, which is favourable in regard of energy consumption.

Acknowledgments

The authors acknowledge the Swiss National Science Foundation and the Swiss Commission of Technology and Innovation (CTI, Bern) for the financial support. The work of Mr. E. Casali for the SSA measurements and Mr. N. Xanthopoulos for the XPS analysis is highly appreciated.

References

[1] S.R. de Miguel, J.I. Vilella, E.L. Jablonski, O.A. Scelza, C. Salinas-Martinez de Lecea, A. Linares-Solano, Appl. Catal. A: Gen. 232 (2002) 237.
[2] R. Fu, Y. Lu, W. Xie, H. Zeng, Carbon 36 (1998) 19.
[3] D.A. Bulushev, L. Kiwi-Minsker, I. Yuranov, E.I. Suvorova, P.A. Buffat, A. Renken, J. Catal. 210 (2002) 149.
[4] M.C. Macias Perez, C. Salinas Martinez de Lecea, A. Linares Solano, Appl. Catal. A: Gen. 151 (1997) 461.
[5] E. Joannet, C. Horny, L. Kiwi-Minsker, A. Renken, Chem. Eng. Sci. 57 (2002) 3453.
[6] J.L. Figueiredo, M.F.R. Pereira, M.M.A. Freitas, J.J.M. Orfao, Carbon 37 (1999) 1379.
[7] M. Domingo-Garcia, F.J.L. Garzon, M.J. Perez-Mendoza, J. Colloid Interface Sci. 248 (2002) 116.
[8] C. Moreno-Castilla, M.V. Lopez-Ramon, F. Carrasco-Marin, Carbon 38 (2000) 1995.
[9] R.-R.F. Radovic, L.R., in: T.P.A. (Ed.), Chemistry and Physics of Carbons, Marcel Dekker, New York, 1997, p. 243.
[10] J.S. Noh, J.A. Schwarz, Carbon 28 (1990) 675.
[11] D.A. Bulushev, I. Yuranov, E.I. Suvorova, P.A. Buffat, L. Kiwi-Minsker, J. Catal. 224 (2004) 8.
[12] G.S. Szymanski, Z. Karpinski, S. Biniak, A. Swiatkowski, Carbon 40 (2002) 2627.
[13] J.M. Calo, D. Cazorla-Amoros, A. Linares-Solano, M.C. Roman-Martinez, C. Salinas-Martinez De Lecea, Carbon 35 (1997) 543.
[14] S. Shin, J. Jang, S.-H. Yoon, I. Mochida, Carbon 35 (1997) 1739.
[15] J.P. Boudou, J.I. Paredes, A. Cuesta, A. Martinez-Alonso, J.M.D. Tascon, Carbon 41 (2003) 41.
[16] J.P. Boudou, A. Martinez-Alonzo, J.M.D. Tascon, Carbon 38 (2000) 1021.
[17] A. Cuesta, A. Martinez-Alonso, J.M.D. Tascon, Carbon 39 (2001) 1135.
[18] M. Domingo-Garcia, F.J. Lopez-Garzon, M. Perez-Mendoza, J. Colloid Interface Sci. 222 (2000) 233.
[19] M. Domingo-Garcia, F.J. Lopez-Garzon, M. Perez-Mendoza, Carbon 38 (2000) 555.
[20] M. Domingo-Garcia, I. Fernandez-Morales, F.J. Lopez-Garzon, C. Moreno-Castilla, M. Pyda, J. Colloid Interface Sci. 176 (1995) 128.
[21] M. Perez-Mendoza, M. Domingo-Garcia, F.J. Lopez-Garzon, Carbon 37 (1999) 1463.
[22] C.U. Pittman Jr., W. Jiang, G.-R. He, S.D. Gardner, Carbon 36 (1998) 25.
[23] J.I. Paredes, A. Martinez-Alonso, J.M.D. Tascon, Carbon 38 (2000) 1183.
[24] J.I. Paredes, A. Martinez-Alonso, J.M.D. Tascon, Carbon 40 (2002) 1101.
[25] J.I. Paredes, A. Martinez-Alonso, J.M.D. Tascon, J. Colloid Interface Sci. 258 (2003) 276.
[26] C. Jones, E. Sammann, Carbon 28 (1990) 509.
[27] C. Jones, E. Sammann, Carbon 28 (1990) 515.
[28] J.-B. Donnet, W.-D. Wang, A. Vidal, M.-J. Wang, Carbon 32 (1994) 199.
[29] K.S. Ahn, J.S. Kim, C.O. Kim, J.P. Hong, Carbon 41 (2003) 2481.
[30] A. Fukunaga, T. Komami, S. Ueda, M. Nagumo, Carbon 37 (1999) 1087.
[31] M. Nakahara, Y. Sanada, Carbon 33 (1995) 735.
[32] A.M. Diamy, Z. Randriamanantenasoa, J.C. Legrand, M. Polisset-Thfoin, J. Fraissard, Chem. Phys. Lett. 269 (1997) 327.
[33] J.-C. Legrand, A.-M. Diamy, G. Riahi, Z. Randriamanantenasoa, M. Polisset-Thfoin, J. Fraissard, Catal. Today 89 (2004) 177.
[34] T.L.M. Maessen, D.S.L. Bruinsma, H.W. Kouwenhoven, H. van Bekkum, J. Chem. Soc., Chem. Commun. (1987) 1284.
[35] Y. Zhang, W. Chu, W. Cao, C. Luo, X. Wen, K. Zhou, Plasma Chem. Plasma Process. 20 (2000) 137.
[36] E.A. Dadashova, T.V. Yagodovskaya, E.S. Shpiro, L.A. Beilin, V.V. Lunin, V.V. Kiselev, Kinet. Catal. 34 (1993) 670.
[37] J.-W. Shim, S.-J. Park, S.-K. Ryu, Carbon 39 (2001) 1635.
[38] D.J. Suh, T.-J. Park, S.-K. Ihm, Carbon 31 (1993) 427.
[39] Y. Otake, R.G. Jenkins, Carbon 31 (1993) 109.
[40] U. Zielke, K.J. Huttinger, W.P. Hoffman, Carbon 34 (1996) 983.
[41] B. Marchon, J. Carrazza, H. Heinemann, G.A. Somorjai, Carbon 26 (1988) 507.
[42] D. Youxian, W. Dianxun, S, Mujin, C Chuanzheng, Y. Jin, Compos. Sci. Technol. 30 (1987) 119.
[43] D.T. Cronce, A.N. Mansour, R.P. Brown, B.C. Beard, Carbon 35 (1997) 483.
[44] A.E. Aksoylu, M. Madalena, A. Freitas, M.F.R. Pereira, J.L. Figueiredo, Carbon 39 (2001) 175.